

This article was downloaded by:

On: 14 January 2011

Access details: *Access Details: Free Access*

Publisher *Taylor & Francis*

Informa Ltd Registered in England and Wales Registered Number: 1072954 Registered office: Mortimer House, 37-41 Mortimer Street, London W1T 3JH, UK



## Molecular Simulation

Publication details, including instructions for authors and subscription information:

<http://www.informaworld.com/smpp/title~content=t713644482>

### Mesoscopic simulation study on the efficiency of surfactants adsorbed at the liquid/liquid interface

Y. Li<sup>a</sup>; X. J. He<sup>a</sup>; X. L. Cao<sup>b</sup>; Y. H. Shao<sup>a</sup>; Z. Q. Li<sup>b</sup>; F. L. Dong<sup>a</sup>

<sup>a</sup> Department of Chemistry and Chemical Engineering, Shandong University, Jinan, P R China <sup>b</sup> Geological Scientific Research Institute, Shengli Oilfield, Dongying, P R China

**To cite this Article** Li, Y. , He, X. J. , Cao, X. L. , Shao, Y. H. , Li, Z. Q. and Dong, F. L.(2005) 'Mesoscopic simulation study on the efficiency of surfactants adsorbed at the liquid/liquid interface', *Molecular Simulation*, 31: 14, 1027 — 1033

**To link to this Article:** DOI: 10.1080/08927020500411948

**URL:** <http://dx.doi.org/10.1080/08927020500411948>

PLEASE SCROLL DOWN FOR ARTICLE

Full terms and conditions of use: <http://www.informaworld.com/terms-and-conditions-of-access.pdf>

This article may be used for research, teaching and private study purposes. Any substantial or systematic reproduction, re-distribution, re-selling, loan or sub-licensing, systematic supply or distribution in any form to anyone is expressly forbidden.

The publisher does not give any warranty express or implied or make any representation that the contents will be complete or accurate or up to date. The accuracy of any instructions, formulae and drug doses should be independently verified with primary sources. The publisher shall not be liable for any loss, actions, claims, proceedings, demand or costs or damages whatsoever or howsoever caused arising directly or indirectly in connection with or arising out of the use of this material.

# Mesoscopic simulation study on the efficiency of surfactants adsorbed at the liquid/liquid interface

Y. LI<sup>†</sup>, X. J. HE<sup>†\*</sup>, X. L. CAO<sup>‡</sup>, Y. H. SHAO<sup>†</sup>, Z. Q. LI<sup>‡</sup> and F. L. DONG<sup>†</sup>

<sup>†</sup>Department of Chemistry and Chemical Engineering, Shandong University, Jinan 250100, P R China

<sup>‡</sup>Geological Scientific Research Institute, Shengli Oilfield, Dongying 257015, P R China

(Received October 2005; in final form October 2005)

Surfactant monolayers at the interface between oil and water has been simulated using dissipative particle dynamics (DPD) technique. With a simple coarse-grained model, how variations in structure of surfactants influence their ability to reduce the interfacial tension has been investigated. The result shows that strong hydrophilic head groups are beneficial to make surfactant molecules more stretched and ordered, and help to enhance the efficiency of surfactant at the interface, it is beneficial to decrease interfacial tension if the hydrophobic chains of the surfactant and the oil have similar structure, and phenyl has a positive effect on interfacial efficiency. The results are in agreement with experimental and other theoretical work on surfactants.

**Keywords:** Interfacial efficiency; Mesoscopic simulation; Oil–water interface; Interfacial tension

## 1. Introduction

Surfactants are amphiphilic molecules, which lower the interfacial tension between the water and the oil phase by forming a monolayer at the interface. Behaviours of surfactants at the interface play an important role in many industrial processes, such as oil extraction, deterging and foaming processes. When choosing between the many surfactants available, both natural and artificially prepared, or designing new ones, one would often like surfactants which reduce the interfacial tension efficiently by adding as little surfactant as possible. The amount of surfactants required to obtain a given interfacial tension reduction depends on several factors: the efficiency at the interface, the tendency to absorb at interface or to form micelles aggregates. The efficiency of a surfactant is defined as the negative logarithm of the surfactant concentration in bulk needed to reduce the interfacial tension by a given amount [1]. While the efficiency at the interface to reflect the interfacial densities (i.e. molecules per area) required to obtain a given interface effect.

Although, the interfacial tension measurements are relatively straightforward, it is difficult to obtain detailed information on the behaviour of the amphiphilic molecules and their concentration at the interface [2]. Only a few techniques, such as non-linear vibrational

sum-frequency spectroscopy [3–6] and second harmonic generation [7], are available for the investigation of liquid–liquid interface. Therefore, molecular simulation is an attractive alternative to provide additional information on distributions and ordering of the amphiphiles, enhancing our understanding of surfactant efficiency at the interface. In the process of designing or choosing new surfactants, it is valuable to know whether a surfactant is more efficient than another.

With the development of computers, computer simulation has made it possible to study surfactant efficiency at the interface on a molecular level, such as molecular dynamics (MD), which give very detailed information on the monolayers formed, for example, the compressed aqueous alkanoate monolayers [8] and the effect of increasing chain length [9], etc. has been successfully studied. However, the time and length scales accessible to ordinary MD simulations are too short to study some phenomena in surfactant system, such as diffusion to the interface and formation of micelles [10]. In the present paper, a mesoscopic level simulation named dissipative particle dynamics (DPD) [11,12] is used to investigate the orientation of surfactants at the water–oil interface. The simulation strategy is to regard clusters of atoms as single coarse-grained particles or beads. By coarse graining the atoms of a molecular, it can access

\*Corresponding author. Tel.: +86-531-88362009. Fax: +86-531-88564464. Email: hexiujuan@mail.sdu.edu.cn

longer length and time scales. Although, less detailed than MD, DPD still enables a systematic study of the effect of surfactant structure on the interfacial tension. In this paper, the effect of mimic variations in chemical structure, for example, changing hydrophilic head groups or the tail length or adding new functional groups, is studied with a simple model by varying the interaction between the dissipative particles. In particular, we investigate how interfacial efficiency of surfactants is related to molecule ordering at the interface.

## 2. Simulation method and details

### 2.1 Theory in DPD

With a bead-spring model, a modified velocity-Verlet algorithm is used to integrate the Newton's equations of motion [13]. The DPD beads follow Newton's equation of motion:

$$\frac{dr_i}{dt} = v_i, \quad m_i \frac{dv_i}{dt} = f_i \quad (1)$$

where  $r_i$ ,  $v_i$ ,  $m_i$ ,  $f_i$  are the position, velocity, mass and force of the  $i$  th particle, respectively.

The forces between two particles  $i$  and  $j$  consist of (soft) repulsive conservative forces ( $F_{ij}^C$ ), pairwise dissipation forces ( $F_{ij}^D$ ) and pairwise random forces ( $F_{ij}^R$ ). The force acting on a particle  $i$  is given by:

$$f_i = \sum_{j \neq i} (F_{ij}^C + F_{ij}^D + F_{ij}^R) \quad (2)$$

with

$$F_{ij}^C = a_{ij}(1 - r_{ij})\hat{r}_{ij} \quad (3)$$

$$F_{ij}^D = -\gamma\omega^D(r_{ij})(\hat{r}_{ij}v_{ij})\hat{r}_{ij} \quad (4)$$

$$F_{ij}^R = \sigma\omega^R(r_{ij})\xi_{ij}\hat{r}_{ij} \quad (5)$$

Here,  $v_{ij}$  is the velocity vector between particle  $i$  and  $j$ ,  $r_{ij}$  is the distance vector between two particles,  $\hat{r}_{ij} = r_{ij}/|r_{ij}|$ .  $\xi_{ij}$ , a number between 0 and 1, is a randomly fluctuating variable with Gaussian statistics.  $a_{ij}$ ,  $\gamma$  and  $\sigma$  determine the amplitude of the conservative, dissipative, and random forces, respectively. The weights  $\omega^D(r_{ij})$  and  $\omega^R(r_{ij})$ , and the amplitudes  $\gamma$  and  $\sigma$  of the dissipative and the random forces have to obey equation (6) [12]

$$\omega^D(r) = [\omega^R(r)]^2, \quad \sigma^2 = 2\gamma k_B T \quad (6)$$

All three above-mentioned forces incline to 0 when the distance between two particles is larger than the cut-off radius. Throughout this paper we use reduced units.  $r_c$  is the units of length,  $k_B T$  (the temperature of the thermostat) is the units of energy, and the mass unit is the mass of a DPD bead. In these units,  $\sigma = 3.0$  and  $\gamma = 4.5$ .

The interfacial tension is defined by the difference in normal and tangential stress across the interface. In the case of a DPD simulation resulting in an interface normal to the  $x$ -axis of the simulation cell, equation (7) [13]

$$\sigma = \int \left[ P_{xx}(x) - \frac{1}{2}(P_{yy}(y) + P_{zz}(z)) \right] dx \quad (7)$$

### 2.2 Model and simulation details in DPD

Different features of surfactant structure have been investigated by changing the hydrophilic head and adding a phenyl group to the linear alkanesulfonates. Also, the influence of the relationship between oils and hydrophobic tail of surfactants on interfacial efficiency has been discussed. The names of the surfactants yield information about their structure: hydrophilic head group is given  $H$ , hydrophobic bead in the tail is given  $T$ , phenyl group  $B$ . For example, alkylbenzenesulfonates surfactants are denoted by  $HBT$  and all other surfactants are regarded as the coarse-grained model of  $HT$ , but they have different repulsion parameters. The effect of variations in structure of surfactants influence can be studied with this model. A surfactant molecule consists of several different beads connected by harmonic springs:

$$f_i^{\text{spring}} = \sum_j C r_{ij} \quad (8)$$

According to Groot and Rabone [14], this condition is met for spring constant  $C = 4$  (in  $kT$  units). Water and oil are represented with a single bead.

It is crucial to calculate the interaction parameters for DPD simulation. They have been obtained by the calculation of the mixing energy of two corresponding fragments represented by DPD beads. The mixing energy of two fragments  $i$  and  $j$   $E_{\text{mix}}^{ij}(T)$  is obtained from the equation as follows [15,16]:

$$E_{\text{mix}}^{ij}(T) = \frac{1}{2} [Z_{ij}\langle E_{ij}(T) \rangle + Z_{ji}\langle E_{ji}(T) \rangle - Z_{ii}\langle E_{ii}(T) \rangle - Z_{jj}\langle E_{jj}(T) \rangle] \quad (9)$$

$Z_{ij}$ ,  $Z_{ji}$ ,  $Z_{ij}$  and  $Z_{jj}$  are the coordination numbers for each pair of beads.  $\langle E_{ij}(T) \rangle$  et al. are the mean pair interaction energy. They have been obtained from Monte-Carlo calculations according to equation (10).

$$\langle E_{ij}(T) \rangle = \frac{\int dE_{ij} P(E_{ij}) E_{ij} \exp(-E_{ij}/kT)}{\int dE_{ij} P(E_{ij}) \exp(-E_{ij}/kT)} \quad (10)$$

$P(E_{ij})$  represents the probability distribution of pair-interaction energies. All the calculated values can be obtained by the use of PCFF force field and Monte-Carlo method on a full atom level, which were performed by Cerius<sup>2</sup> software on the SGI workstation. Then, the Flory-Huggins interaction parameters  $\chi_{ij}(T)$  can be plotted as a function of temperature from the model

$E_{\text{mix}}^{ij}(T)$  data. The relationship between them was described as the following equation:

$$\chi_{ij}(T) = \frac{E_{\text{mix}}^{ij}(T)}{RT} \quad (11)$$

A linear relation for the repulsion parameters  $a_{ij}$  and the Flory–Huggins interaction parameters  $\chi_{ij}(T)$  is given [17,18], in  $kT$  units:

$$a_{ij} = a_{ii} + \frac{\chi_{ij}(T)}{0.306} = 25 + 3.27\chi_{ij}(T) \quad \rho = 3 \quad (12)$$

Between beads of the same type, the repulsion parameters are taken as  $a_{ii} = 75k_B T / \rho = 25k_B T (\rho = 3)$ , which is derived from the compressibility of water at room temperature.

All simulations have been performed in the NVT-ensemble. For studying interfacial properties expediently, a  $20 \times 10 \times 10$  box containing a total number of 6000 beads ( $\rho = 3$ ) is used. Periodic boundary conditions are applied in all three directions. The surfactants are inserted in the system by replacing  $O$  particles with  $T$  particles and  $W$  particles with  $H$  particles in such a way that the total amount of particles remains constant. The input repulsion parameters are derived from the calculation using the above theories and methods. The DPD simulations run 20,000 steps with a time step of 0.05, evolving to a steady state that corresponds to the Gibbs canonical ensemble. All the simulations are performed using Cerius<sup>2</sup> software on the SGI workstation.

### 3. Results and discussion

The interfacial tension of the system will decrease when the number of surfactants increases. Different surfactants yield different results concerning the lowering of the interfacial tension. The efficiency of a surfactant in experiments is determined by the  $\text{pC}_{40}$  or  $\text{pC}_{20}$ , the negative logarithm of the surfactant concentration needed to reduce the interfacial tension by 40 or 20  $\text{m Nm}^{-1}$  [19]. In this work, the efficiency of a surfactant is determined qualitatively, the surfactant which needs less molecules at the interface to equally reduce the interfacial tension is considered to be more efficient.

In experimental studies of surfactant efficiency, the bulk concentration is determined from the total amount of surfactants added, while molecule simulation can give curves of  $\gamma$  as a function of interfacial density. It has different indications; the former reflects efficiency of a surfactant, while the latter reflects efficiency at the interface. In fact, the latter is even more important to us. In the following sections, three trends in structure of surfactants on influence of interfacial efficiency are studied: the selectivity and adaptability between oils and tail groups of surfactant, changing the hydrophilic head group and adding phenyl groups.

A change in the appearances of the interfaces has been observed when the number of surfactants in the system is

increased. At low surfactant concentrations the interfaces are not completely covered, though all surfactants are located at the interface. Above a certain concentration the interfaces are covered, and the remaining surfactants drift into the water or the oil phase, where they aggregate into micelle-like structures [20].

At a low surfactant concentration the surfactants have interaction with the water and the oil phase only, thus the location at the interface is the most favourable. At high surfactant concentrations the surfactants at the interface will have interaction with each other, which causes some surfactants to move away from the interface and cluster together in micelle-like structures.

For each simulation the interfacial tension is averaged over the sampling cycles. For all studied surfactants it is observed that the interfacial tension decreases as the number of surfactants increases until it comes to the minimum.

#### 3.1 Comparison of linear alkanesulfonate and linear alkylbenzenesulfonate surfactants

Linear alkanesulfonates and alkylbenzenesulfonates constitute a large fraction of the surfactants used in commercial detergents and cleansers. Despite the industrial significance and the possible environmental impact of these compounds, very little is known regarding the molecular properties of these compounds and how they relate to macroscopic properties desired in applications. In this section, we employ DPD method to examine and compare the molecular structure of surfactants in these two classes as they adsorb at organic–water interface. The linear alkane- and alkylbenzenesulfonates studied are, respectively, dodecanesulfonate and dodecylbenzenesulfonate. By measurement and comparison of the interfacial properties of these adsorbed surfactants, changes in the interfacial efficiency and the number density of surfactant molecules at the interface are examined.

In DPD simulation, the calculated  $a_{ij}$  parameters by the theories and methods in section 2.2. are given in table 1. Figure 1 shows the reduction of the interfacial tension vs the number of surfactants at interface for linear alkanesulfonate and alkylbenzenesulfonate surfactants. The average number of surfactants at the interface is determined by integrating the average density profiles over the interface. The efficiency of a surfactant is qualitatively determined from the graph in figure 1.

Table 1. The interaction parameters  $a_{ij}$  of dodecanesulfonate and dodecylbenzenesulfonate systems (in  $kT$  units).

$a_{ij}$	$W$	$O$	$H$	$B$	$T$
W	25.0	75.0	9.56	23.6	75.0
O	75.0	25.0	70.9	28.8	25.0
H	9.56	70.9	25.0	19.4	70.9
B	23.6	28.8	19.4	25.0	28.8
T	75.0	25.0	70.9	28.8	25.0

Note: Here,  $H$  represents the head group of the two kinds of surfactants;  $T$  the tail chain;  $B$  the phenyl group;  $W$  the water molecule;  $O$  the oil, dodecane.

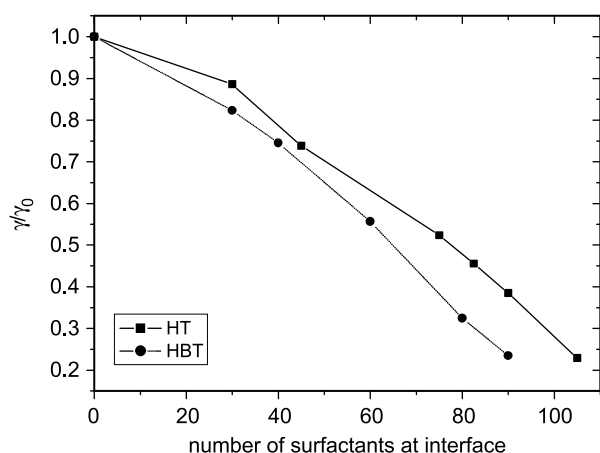


Figure 1. Plot of the relative interfacial tension reduction ( $\gamma/\gamma_0$ ) of dodecanesulfonate and dodecylbenzenesulfonate surfactants vs the number of surfactant at interface. Note: here ( $\gamma_0$ ) is the interfacial tension of the system without surfactant.

It shows that phenyl groups have a positive effect in increasing the interfacial efficiency of a linear sulfonate surfactants. This is in agreement with experimental results done by Watry *et al.* [6].

We attribute this difference in interfacial efficiency to the presence of the benzene ring in dodecylbenzenesulfonate. The existence of the phenyl groups disrupting chain–chain interactions for the first few methylene groups adjacent to the benzene ring in alkylbenzenesulfonate, which appears to result in significantly ordered for alkylbenzenesulfonate at interface. The molecular properties that lead to the high solubility of alkylbenzenesulfonate in water relative to alkanesulfonate seem to also play a role in how these molecules adsorb at a hydrophobic/hydrophilic surface. These might be factors in the difference in interfacial efficiency of these two surfactants.

### 3.2 The effect of the hydrophilic head group on the efficiency at the interface

Molecular structures of different surfactant head groups studied in this section are given in figure 2.

#### 3.2.1 The interaction parameters in DPD simulation.

In DPD simulation, the parameters between water (W) and the head group ( $H_b$ ) is normalized to zero interaction. This is the strongest attractive interaction among DPD particle pairs. The calculated  $a_{ij}$  parameters are given in table 2. We can clearly see that although all the head groups are regarded as the coarse-grained model of  $H$ , they have different repulsion parameters.

**3.2.2 The interfacial efficiency.** In figure 3A the relative interfacial tension reduction is plotted as a function of the number of surfactants at the interface.

The difference in efficiency between the different surfactants is not very clear at a low number of surfactants at the interface. The surfactants only have interaction with

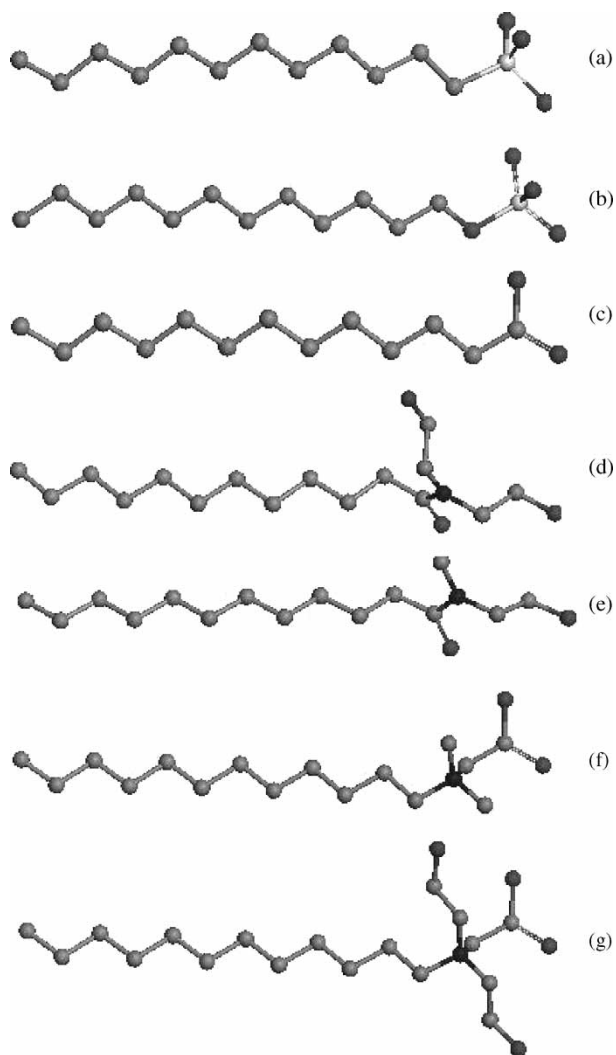


Figure 2. Molecular structures of different surfactants.

the water and the oil phase, not with each other. At a high concentration the difference in efficiency becomes more apparent, due to the interaction of the surfactants with each other.

Figure 3 shows that alkanesulfate and alkanesulfonate surfactants have the greatest interfacial efficiency, while that of alkanecarboxylate surfactants are the lowest. At the liquid–liquid interface, the van der Waals attractions are reduced as solvent is introduced between the tail chains. Thus the interaction relating to head groups is crucial for the orientation of surfactants, since all the surfactants have the same tail chains. Therefore, the difference can be explained that the sulfate and sulfonate head groups are more hydrophilic than the carboxylate heads. We can see it from the interaction parameters  $a_{ij}$  in table 2. The former have lower head–water repulsion parameters and higher oil–head repulsion.

According to Conboy *et al.* [21], the solvation of ionic head group promotes the adsorption of surfactants through the variation of the penetration depth and interfacial roughness. With the solvation of ionic head groups, the tendency for the head groups to be surrounded by water



Table 2. The interaction parameters  $a_{ij}$  of simulation systems (in  $k_B T$  units).

$a_{ij}$	W	O	T	$H_a$	$H_b$	$H_c$	$H_d$	$H_e$	$H_f$	$H_g$
W	25.0	75.0	75.0	9.56	0.0	37.6	31.9	19.3	16.5	33.5
O	75.0	25.0	25.0	70.9	101.3	81.0	125.5	103.0	100.8	87.6
T	75.0	25.0	25.0	70.9	101.3	81.0	125.5	103.0	100.8	87.6
$H_a$	9.56	70.9	70.9	25.0	—	—	—	—	—	—
$H_b$	0.0	101.3	101.3	—	25.0	—	—	—	—	—
$H_c$	37.6	81.0	81.0	—	—	25.0	—	—	—	—
$H_d$	31.9	125.5	125.5	—	—	—	25.0	—	—	—
$H_e$	19.3	103.0	103.0	—	—	—	—	25.0	—	—
$H_f$	16.5	100.8	100.8	—	—	—	—	—	25.0	—
$H_g$	33.5	87.6	87.6	—	—	—	—	—	—	25.0

Note:  $H$  represents different head groups,  $T$  the tail chain,  $W$  the water molecule and  $O$  dodecane,  $O$  and  $T$  here represents the same beads.

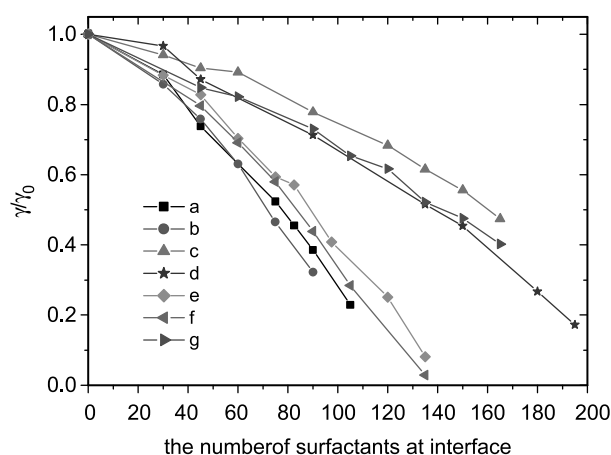


Figure 3. Plot of the relative interfacial tension reduction ( $\gamma/\gamma_0$ ) vs the number of surfactants at dodecane–water interface.

rather than other head groups is enhanced. They penetrate into the water phase, making the effective chain length in the oil phase reduced, then gauche defects become less. Simultaneously, the strong attractive interaction between head group and water reduces the wiggle of chain, and the conformational instability of the alkyl chains can be reduced. Therefore, these molecules are more stretched and ordered at the interface as shown in figure 4 [20], thus

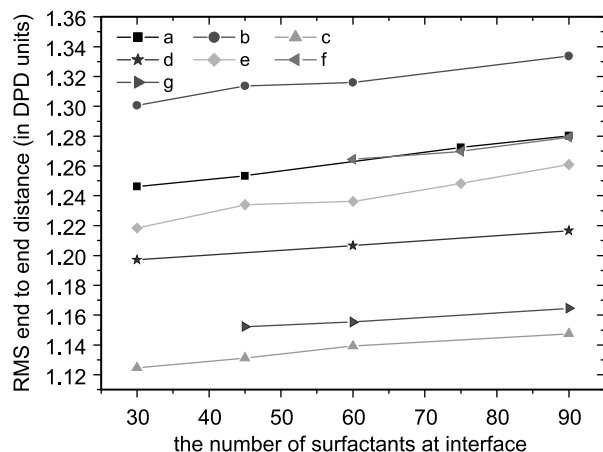


Figure 4. RMS end-to-end distance of the surfactants at the oil–water interface under different concentrations.

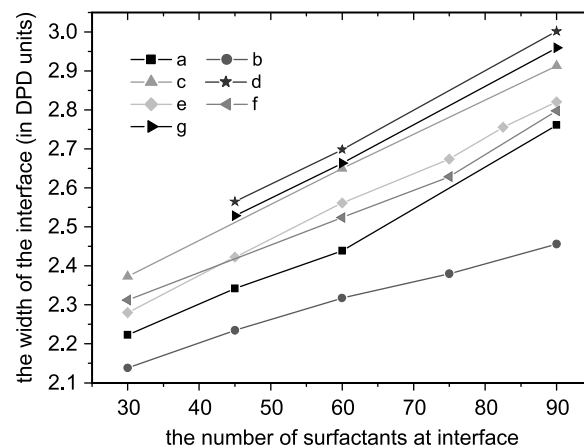


Figure 5. The width of the surfactants distribution at the oil–water interface (it is defined to be the distance between two positions where the density varies from 10 to 90% of that of the bulk phase [22]).

increases their efficiency at interface in lowering the interfacial tension.

An increase in the oil–head repulsion decreases the oil solubility of the surfactant. Investigations of the density profiles show that the surfactants with higher oil–head repulsion stagger less at the interface, as demonstrated by the narrower distribution of the surfactants at the interface in figure 5 (the staggered surfactants are still at the interface, only arranged in a way which reduces the interfacial tension less than those that are more aligned). By such an arrangement, the effective lateral repulsion increases, yielding higher surface pressure and efficiency.

### 3.3 The influence of the relationship between oils and hydrophobic tail of surfactants

Interfacial tension measurements showed that there are a certain relation between hydrophobic tail groups of surfactants and oils. According to literature, under the condition that the constitute and concentration of surfactants are fixed, with the alkane hydrocarbon of the different carbon atomicity for the oil, the interface tension of the oil–water–surfactant system changes with the change of the number of the carbon atoms of the alkane hydrocarbon. At a certain carbon atomicity, it comes to the lowest. This carbon's atomicity is known as optimal

Table 3. The interaction parameters  $a_{ij}$  of simulation systems (in  $k_B T$  units).

$a_{ij}$	$W$	$H$	$o$	$d$	$h$
W	25.0	9.56	65.1	75.0	98.3
H	9.56	25.0	22.8	70.9	93.9
o	65.1	22.8	25.0	28.0	48.9
d	75.0	70.9	28.0	25.0	33.9
h	98.3	93.9	48.9	33.9	25.0

Note: Here,  $H$  represents the head group;  $W$  the water molecule;  $o$  the tail chain or the oil, octane;  $d$ , dodecane and  $h$ , hexadecane.

carbon number opposite to oil of the system. In this section, the mesoscopic simulation is used to investigate the influence of this kind of relation on the efficiency of alkanesulfonate surfactant at interface. The calculated  $a_{ij}$  parameters are shown in table 3.

In figure 6, the ratio of the interfacial tension ( $\gamma/\gamma_0$ ) of different surfactants are plotted as a function of the interfacial density for different systems, respectively. The result shows that for octane–water systems, surfactant  $C_8H$  is the most efficient in decreasing interfacial tension, while for dodecane–water systems, surfactant  $C_{12}H$  is the best and hexadecane–water systems, it is  $C_{16}H$ . So we can clearly see that it is beneficial to increase interfacial efficiency if the length of the hydrophobic chain of the surfactant is equal to that of oil.

In order to understand why the surfactants whose hydrophobic chain have similar structure with the oil are more efficient in decreasing interfacial tension than other surfactants, the RMS end-to-end distance of the surfactants at the interface are investigated.

In figure 7, the RMS end-to-end distance of the surfactants are plotted as a function of the number of it at the interface. The graphs in figure 7 show that surfactant are more ordered and stretched than others if the length of the hydrophobic chain is similar to that of oil. Thus increases the efficiency at the interface.

#### 4. Conclusions

In a mixture of oil and water the interfacial tension is reduced by surfactants, amphiphilic molecules. The influence of the structure of these surfactants on decreasing interfacial tension is studied with a simulation technique called dissipative particle dynamics. Three aspects have been studied: different head groups of surfactant, the selectivity and adaptability between surfactant and oil, and the influence of phenyl on interfacial efficiency.

We found that lower concentrations of surfactants with strong hydrophilic head groups are required to obtain the same reduction of the interfacial tension of an oil–water system. We argue that the stronger interactions make them more stretched at the interface, thus make these surfactants more efficient at the interface. It is beneficial to decrease interfacial tension if the hydrophobic chains of the surfactant and the oil have similar structure, for the molecule at interfacial layer could array compactly.

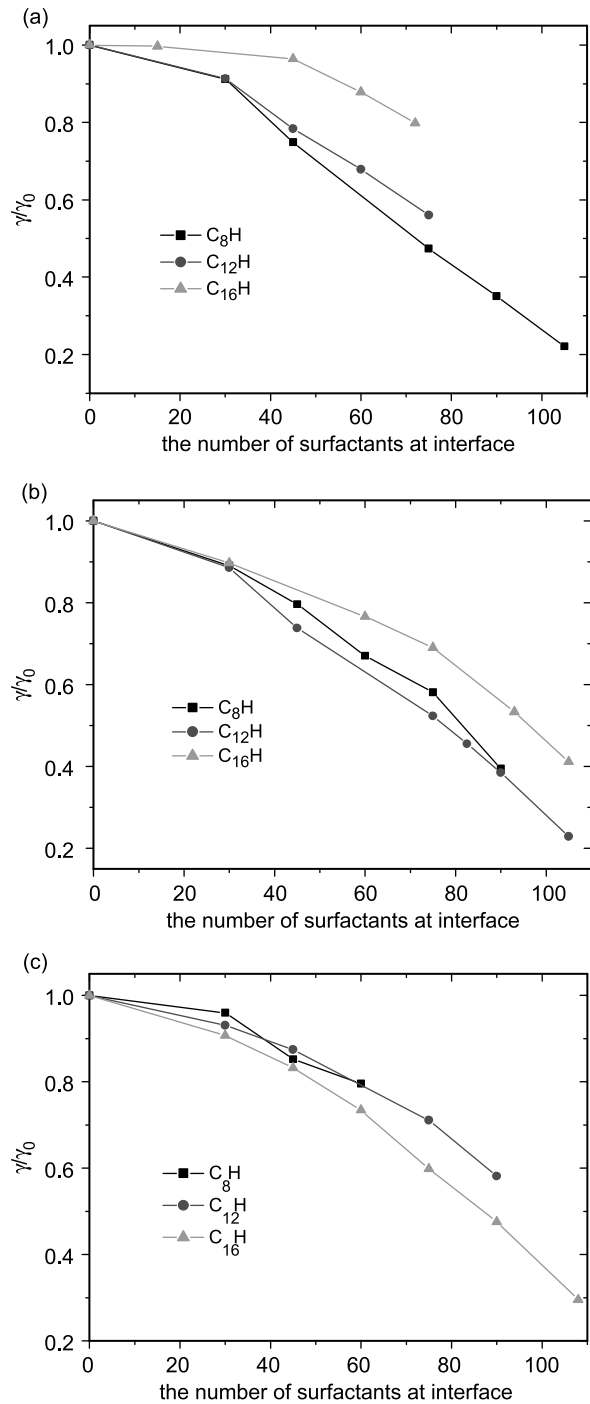


Figure 6. Plot of the relative interfacial tension reduction ( $\gamma/\gamma_0$ ) of different surfactants vs the number of surfactants at interface: octane–water system (a); dodecane–water system (b); hexadecane–water system (c).

Another important phenomenon is that phenyl group has a positive effect on interfacial efficiency, because the monolayer formed by these surfactants is more ordered. The results are in agreement with experimental and other theoretical work on surfactants.

We have shown that DPD simulations of simple oil–water-surfactant systems can predict surfactant behaviour at interfaces. It might be an attractive method to analysis

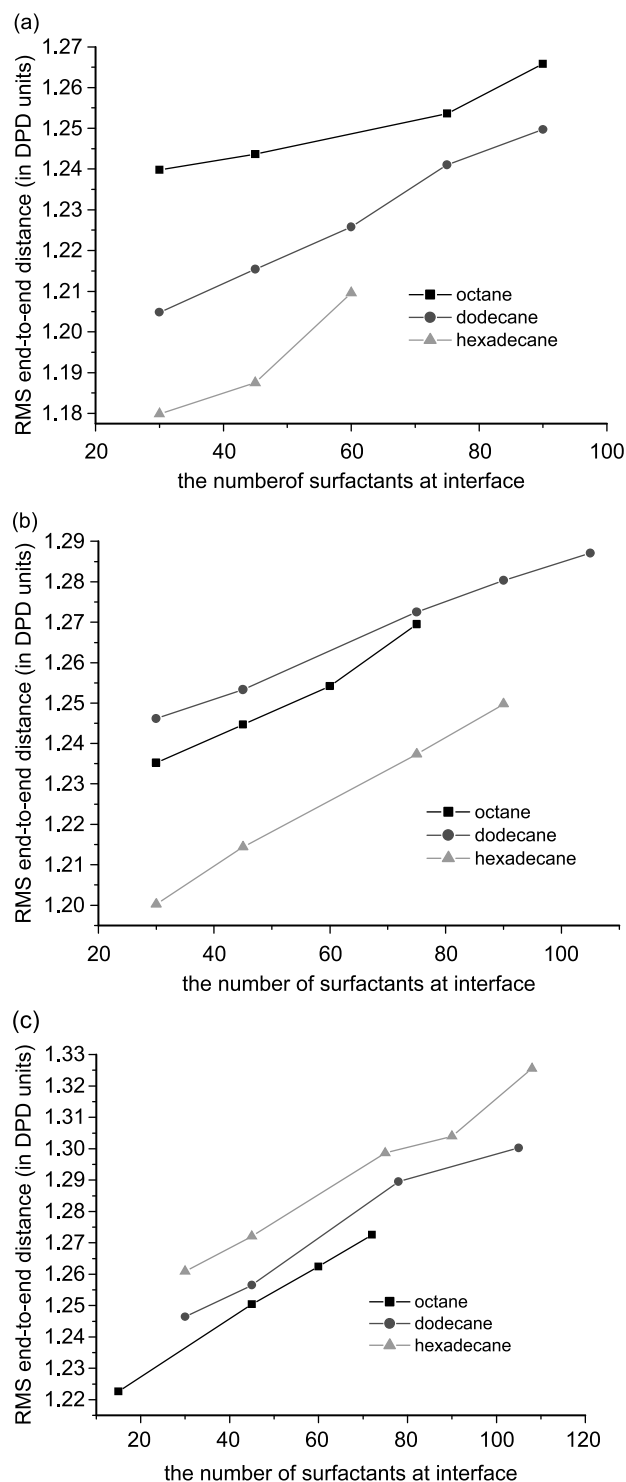


Figure 7. The influence of oil on RMS end-to-end distance of three surfactants  $C_8H$  (a)  $C_{12}H$  (b)  $C_{16}H$  (c) at different concentrations.

of the efficiency of the surfactants, guiding its applications in actual industry.

## Acknowledgements

This work was supported from the National Natural Science Foundation of China (No. 29903006).

## References

- [1] M.J. Rosen. *Surfactants and Interfacial Phenomena*, 2nd ed., 0-471-47818-0, Wiley, New York (1989).
- [2] J.R. Lu, R.K. Thomas, J. Penfold. Surfactant layers at the air/water interface: structure and composition. *Adv. Colloid Interface Sci.*, **84**, 143 (2000).
- [3] M.C. Messmer, J.C. Conboy, G.L. Richmond. Observation of molecular ordering at the liquid-liquid interface by resonant sum frequency generation. *J. Am. Chem. Soc.*, **117**, 8039 (1995).
- [4] J.C. Conboy, M.C. Messmer, G.L. Richmond. Dependence of alkyl chain conformation of simple ionic surfactants on head group functionality as studied by vibrational sum-frequency spectroscopy. *J. Phys. Chem. B.*, **101**, 6724 (1997).
- [5] J.C. Conboy, M.C. Messmer, G.L. Richmond. Effect of alkyl chain length on the conformation and order of simple ionic surfactants adsorbed at the  $D_2O/CCl_4$  interface as studied by sum-frequency vibrational spectroscopy. *Langmuir*, **14**, 6722 (1998).
- [6] M.R. Watry, G.L. Richmond. Comparison of the adsorption of linear alkanesulfonate and linear alkylbenzenesulfonate surfactants at liquid interfaces. *J. Am. Chem. Soc.*, **122**, 875 (2000).
- [7] S.G. Grubb, M.W. Kim, T. Rasing, Y.R. Shen. Orientation of molecular monolayers at the liquid-liquid interface as studied by optical second harmonic generation. *Langmuir*, **4**, 452 (1988).
- [8] Ciara Bergin, D.A. Morton-Blake. A molecular dynamics investigation of compressed aqueous alkanoate monolayers. *Mol. Simul.*, **29**, 535 (2003).
- [9] B. Smit, A.G. Schlijper, L.A.M. Rupert, N.M. van Os. Effects of chain length of surfactants on the interfacial tension: molecular dynamics simulations and experiments. *J. Phys. Chem.*, **94**, 6933 (1990).
- [10] S.J. Marrink, D.P. Tieleman, A.E. Mark. Molecular dynamics simulation of the kinetics of spontaneous micelle formation. *J. Phys. Chem. B*, **104**, 12165 (2000).
- [11] P.J. Hoogerbrugge, J.M.V.A. Koelman. Simulating microscopic hydrodynamic phenomena with dissipative particle dynamics. *Europhys. Lett.*, **19**, 155 (1992).
- [12] P. Espagnol, P. Warren. Statistical mechanics of dissipative particle dynamics. *Europhys. Lett.*, **30**, 191 (1995).
- [13] R.D. Groot, P.B. Warren. Dissipative particle dynamics: bridging the gap between atomistic and mesoscopic simulation. *J. Chem. Phys.*, **107**, 4423 (1997).
- [14] R.D. Groot, K. Rabone. Mesoscopic simulation of cell membrane damage, morphology change and rupture by nonionic surfactants. *Biophys. J.*, **81**, 725 (2001).
- [15] E. Ryjkina, H. Kuhn, H. Rehage, F. Muller, J. Peggau. Molecular dynamic computer simulations of phase behavior of non-ionic surfactants. *Angew. Chem. Int. Ed.*, **41**, 983 (2002).
- [16] M.Y. Kuo, H.C. Yang, C.Y. Hua, C.L. Chen. Computer simulation of ionic and nonionic mixed surfactants in aqueous solution. *Chem. Phys. Chem.*, **5**, 575 (2004).
- [17] R.D. Groot. Mesoscopic simulation of polymer-surfactant aggregation. *Langmuir*, **16**, 7493 (2000).
- [18] R.D. Groot. Electrostatic interactions in dissipative particle dynamics-simulation of polyelectrolytes and anionic surfactants. *J. Chem. Phys.*, **118**, 11265 (2003).
- [19] M. Rosen, A. Cohen, M. Dahanayake, X.-Y. Hua. Relationship of structure to properties in surfactants: Surface and thermodynamic properties of 2-dodecyloxy poly(ethenoxyethanol)s,  $C_{12}H_{25}(OC_2H_4)_xOH$ , in aqueous solution. *J. Phys. Chem.*, **86**, 541 (1982).
- [20] L.D. Feng, L. Ying, Z. Peng. Mesoscopic simulation study on the orientation of surfactants adsorbed at the liquid/liquid interface. *Chem. Phys. Lett.*, **399**, 215 (2004).
- [21] H. Kuhn, H. Rehage. Molecular orientation of monododecyl pentaethylene glycol at water/air and water/oil interfaces. A molecular dynamics computer simulation study. *Colloid. Polym. Sci.*, **278**, 114 (2000).
- [22] S.J. Seung, T.L. Shiang, K.M. Prabal. Molecular dynamics study of a surfactant-mediated decane-water interface: effect of molecular architecture of alkyl benzene sulfonate. *J. Phys. Chem. B.*, **108**, 12130 (2004).